

Article

A Novel Trinuclear Nickel(II) Salicylaldimine Complex: Synthesis, Structural Characterization, Bioactivity Profile against Bacterial, Fungal and Breast Cancer Cells and Effects on Wheat Germination Indices

Ereny S. Williem¹, Ahmed Amro² , Ahmed B. M. Ibrahim^{3,*} , S. Abd Elkhaliq¹, Peter Mayer⁴ and S. M. Abbas¹ 

¹ Chemistry Department, Faculty of Science, Beni-Suef University, Beni-Suef 62521, Egypt; ereny.samy@science.bsu.edu.eg (E.S.W.); sawsan.abdelhalik@science.bsu.edu.eg (S.A.E.); safaa.mohammed@science.bsu.edu.eg (S.M.A.)

² Botany and Microbiology Department, Faculty of Science, Assiut University, Assiut 71516, Egypt

³ Department of Chemistry, Faculty of Science, Assiut University, Assiut 71516, Egypt

⁴ Department Chemie, Ludwig-Maximilians-Universität München, Butenandtstr. 5-13, Haus D, 81377 München, Germany; pemay@cup.uni-muenchen.de

* Correspondence: aibrahim@aun.edu.eg

Abstract: The complex $[\text{Ni}_3\text{L}_6] \cdot 1.56\text{CH}_2\text{Cl}_2$ (**HL** = (*E*)-2-(((3,4-dimethylphenyl)imino)methyl)phenol) was isolated in the monoclinic *C* 2/*c* space group. All nickel atoms are six-coordinate with a nickel atom bound to only O-phenol atoms, while the two terminal cations are surrounded by N_3O_3 atoms. This complex and its ligand (20 mg/mL in DMSO) were tested as antimicrobials. Against two fungi, the complex and amphotericin B caused 13 and 21 mm inhibition diameters, respectively, in *Candida albicans* plates. Against four bacteria, the ligand inhibited only *Staphylococcus aureus* with a 10 mm diameter, and the complex induced inhibitions with 10–13 mm (ampicillin afforded 21–26 mm inhibitions). Against cancer (MCF-7) and normal (BHK) cells, the ligand provided virtual inactivity, but great activities ($\text{IC}_{50} = 5.44$ and $11.61 \mu\text{M}$, respectively) were shown by the complex. Doxorubicin afforded activities with $\text{IC}_{50} = 9.66$ and $36.42 \mu\text{M}$ in these cells, respectively. The ligand and its complex offered 100% germination of a drought-sensitive wheat cultivar (90% for control), but, under drought, the complex, ligand and control gave germination with 85, 75 and 95%, respectively. Under normal irrigation and drought, the control and complex afforded 100% germination, and the ligand afforded 95% germination for a drought-resistive wheat cultivar.

Keywords: Schiff base; anionic ligands; *Candida albicans*; MCF-7; cultivar; *Staphylococcus aureus*



Citation: Williem, E.S.; Amro, A.; Ibrahim, A.B.M.; Abd Elkhaliq, S.; Mayer, P.; Abbas, S.M. A Novel Trinuclear Nickel(II) Salicylaldimine Complex: Synthesis, Structural Characterization, Bioactivity Profile against Bacterial, Fungal and Breast Cancer Cells and Effects on Wheat Germination Indices. *Crystals* **2023**, *13*, 1084. <https://doi.org/10.3390/cryst13071084>

Academic Editors: Ezzat Khan and Awal Noor

Received: 25 June 2023

Revised: 8 July 2023

Accepted: 10 July 2023

Published: 11 July 2023



Copyright: © 2023 by the authors. Licensee MDPI, Basel, Switzerland. This article is an open access article distributed under the terms and conditions of the Creative Commons Attribution (CC BY) license (<https://creativecommons.org/licenses/by/4.0/>).

1. Introduction

Hugo Schiff (1834–1915) is an Italian–German scientist who succeeded in the preparation of the first Schiff base. Since that time, Schiff base chemistry, with its rich biological and industrial applications, has expanded to represent a very significant research domain [1–3]. The structural varieties on Schiff bases and their properties (e.g., (electro)luminescence) [4–6] enable them for utilization as dyes, pigments, corrosion inhibitors, catalysts, sensors and photovoltaic materials, as well as starting materials for valuable industrial chemicals (through cycloaddition, replacement and ring closure procedures) [7–9]. Further, these compounds, due to pharmacological, biochemical and clinical characteristics, show urease inhibition, antibacterial, DNA interaction, antitumor, hypoglycemic and antifungal properties [10–15]. Moreover, using these compounds, eclectic fluorescence quantification of particular metals (both in vitro and in vivo) in biological media has been reported [16]. Indeed, transition, inner-transition and main group metal complexes with Schiff bases (bi-, tri-

and tetra-dentate through the azomethine (N) and other atoms depending on the ligand substituents) were reported [17]. These complexes, according to their steric, physicochemical, structural and electronic properties, show notable and selective catalytic activities (homogeneous and heterogeneous) frequently in electron transfer reactions [18–20], beside their behavior as dyes [21] and analytical reagents [22], as well as materials for polymeric [23] and energy [24] applications. In addition, they show drug likeness that frequently exceeds the unbound Schiff base action, as proteasome inhibitors, metalloenzymes and antibacterial, anticancer, antifungal and DNA and protein (e.g., bovine serum albumin) binding agents [25–34].

An important class of the Schiff base ligands, derived from reactions between primary amines and salicylaldehydes, is the salicylaldimines [35,36]. These flexidentate ligands form complexes with tuned redox, magnetic and spectral characteristics with regard to the metals [37,38]. Hence, the metal salicylaldimines present efficient oxygenation and asymmetric catalytic activities and ability for building liquid crystals and various supramolecular architectures [39–44]. From another side, nickel is an important element, as its compounds are excellent catalysts for oxidation and olefin polymerization [45–47]. Biologically, no Ni(II) drugs are commercialized [48], but nickel is essential for some microorganisms, animals and plants [49]. This element is a fundamental component in the enzymes acetyl-CoA decarboxylase/synthase, Ni-Fe hydrogenase, urease, CO dehydrogenase, various glyoxylases and superoxide dismutases, methyl coenzyme M reductase, methylenediurease and acireductone dioxygenase [50–52]. Nickel is also present in the nucleic acids (RNA and DNA) and breast milk [53,54]. Moreover, it enhances iron absorption, red blood cells' production and the adrenaline and glucose metabolism [53,54]. Indeed, some Ni(II) compounds were used to mimic enzymes [55] and to cause cleavage of plasmid DNA [56].

Here, we introduce a centrosymmetric trinuclear nickel salicylalimine complex involving the ligand (*E*)-2-(((3,4-dimethylphenyl)imino)methyl)phenol. Following its spectral and solid state structure characterization, this paper uncovers the antibacterial (in *S. aureus*, *B. subtilis*, *E. coli* and *P. aeruginosa* cultures) and antifungal (in *A. flavus* and *C. albicans* cultures) activities of the unbound ligand and its complex, compared with ampicillin and amphotericin B, respectively. Moreover, the cytotoxic effects by these compounds on human breast MCF-7 cancer cells and normal baby hamster kidney (BHK) cells, comparing with doxorubicin, were studied to indicate the utility of these compounds in cancer chemotherapy. Finally, to detect how these compounds find usefulness in agricultural fields, we investigated their influence on the germination of wheat cultivars with drought-sensitive and drought-resistive properties.

2. Materials and Methods

2.1. Chemicals and Instruments

Hexahydrated nickel chloride (MERCK, Rahway, NJ, USA), 3,4-dimethylaniline (Sigma-Aldrich, Burlington, MA, USA) and salicylaldehyde (Alfa Aesar, Ward Hill, MA, USA) were provided with highest purity to be involved in the reactions as obtained. Absolute ethanol and dichloromethane for the complex synthesis were commercially supplied. All synthetic procedures were with no exclusion of air. Ambient room conditions applied during the analysis and experiments, unless stated otherwise. Microanalysis for the elements (carbon, hydrogen and nitrogen) was performed with a Vario EL III analyzer. Solution electrical conductivity of the nickel complex in dimethylformamide was measured using a Jenway 4320 conductivity meter. The ligand and complex UV-visible absorption spectra were determined in DMSO with a Perkin-Elmer Lambda 40 UV/VIS spectrometer, but their Fourier transform infrared spectra (both pressed in KBr disks) were acquired with a Nicolet iS10 spectrometer. A crystal of the nickel complex with the dimensions $0.196 \times 0.103 \times 0.080$ mm was selected for X-ray single crystal diffraction study at 120(2) K on a Bruker D8 Venture Kappa Duo apparatus supplied with a multilayer mirror monochromator alongside a rotating anode X-ray tube for MoK α radiation of $\lambda = 0.71073$ Å. The Bruker SAINT software package [57] and the Multi-Scan method (SADABS) [58] were

respectively used for the frames' integration and for the data correction for absorption effects, respectively. The crystal structure was both solved and refined with the Bruker SHELXTL Software Package [59]. All hydrogen atoms were specified in supreme geometry according to their parent atoms. Disorder of dichloromethane has been described by a split model. The site occupation factors of the two disordered parts refined to 0.65 and 0.13. The carbon–chlorine bonds have been restrained to be equal within a standard deviation of 0.01 Å, while the chlorine–chlorine distances have been restrained to be equal within a standard deviation of 0.02 Å. The SIMU restraint has been applied to improve displacement parameters of disordered atoms with distances closer than 0.8 Å. The programs ORTEP-3 [60] and Mercury 2020 [61] were used for drawing the complex crystal structure and packing scheme with a 50% ellipsoid probability level, respectively. Crystallographic data, as well as details on data collection and structure solution and refinement parameters, are listed in Table 1.

Table 1. Crystallographic and structure refinement information for the nickel complex.

Empirical formula	C _{91.56} H _{87.12} Cl _{3.12} N ₆ Ni ₃ O ₆	shift/error _{max}	0.002
Formula weight	1654.21	θ range for data collection (°)	1.929–27.497
Crystal system	Monoclinic	Reflections measured	75,494
space group	C 2/c	Reflections in refinement	9033
a (Å)	25.2766(15)	Observed reflections	8263
b (Å)	13.3628(9)	R _{int}	0.0290
c (Å)	25.3398(18)	Parameters (Restraints)	536 (25)
α (°)	90	Transmission factor range	0.89–0.93
β (°)	113.128(2)	GOF on F ²	1.074
γ (°)	90	R (F _{obs})	0.0311
Volume (Å ³)	7871.0(9)	mean σ(I)/I	0.0149
Z	4	R _w (F ²)	0.0801
Density (g/cm ³)	1.396	Largest diff. peak, hole/e Å ⁻³	0.868, −0.387
μ (mm ⁻¹)	0.876	x, y (weighting scheme)	0.0313, 13.4093

2.2. The Complex Synthesis

Caution was required, as 3,4-dimethylaniline is toxic to humans and should be handled with care. The ligand was synthesized via condensation of salicylaldehyde and 3,4-dimethylaniline according to the literature method [62]. To a quantity of 1 mmol of HL (225 mg) dissolved in warm ethanol (10 mL) containing 0.2 mL of triethylamine, NiCl₂·6H₂O (119 mg, 0.5 mmol) was added under stirring. A green solid appeared instantly, and was left to stir in the medium for 15 min before its recovery by filtration and washing with ethanol. After drying in the air, this solid was added to dichloromethane (20 mL) under stirring, and any undissolved particles were discarded by filtration. The clean filtrate was left for slow evaporation in the air for 24 h, whereupon green single crystals of the complex were separated, collected by filtration, washed with ethanol and air dried.

[Ni₃L₆]•1.56CH₂Cl₂ **C1**: Yield = 251 mg (91%). Anal. Calcd. (Found) for C_{91.56}H_{87.12}Cl_{3.12}N₆Ni₃O₆ (MW = 1654.21 g/mol), C = 66.48 (66.06)%, H = 5.32 (5.35)% and N = 5.08 (5.18)%. FT-IR (KBr, cm⁻¹) = 1607 ν(CH=N), 573 ν(Ni—O) and 452 ν(Ni—N). Electronic (DMSO, nm) = 340 and 607. Λ (DMF, Ω⁻¹cm²mol⁻¹) = 12.14.

2.3. In Vitro Antimicrobial Activity Assay

The antimicrobial activity against Gram-positive bacteria (*Bacillus subtilis* ATCC 6051 and *Staphylococcus aureus* ATCC 12600), Gram-negative bacteria (*Escherichia coli* ATCC 11,775 and *Pseudomonas aeruginosa* ATCC 10145) and fungi (*Aspergillus flavus* ATCC 9643 and *Candida albicans* ATCC 10231) was screened. The microbes were provided from the American Type Culture Collection (ATCC, Alexandria, MN, USA) and their inhibitions, by HL and the nickel complex comparing with ampicillin (antibacterial) and amphotericin B

(antifungal) standards, were thrice recorded via a detailed method [63]. Briefly, all bacteria were grown on broth nutrient agars and the fungi were grown on Sabouraud dextrose agars. From each microbe, 100 microliters were moved to fresh media (10 mL) until the counts reached 5×10^8 bacteria/mL, 5×10^3 *Aspergillus flavus*/mL and 5×10^5 *Candida albicans*/mL. Bacterial and fungal suspensions (100 μ L) were moved onto new agars of similar composition, and incubation of all species was further occurred (for *Aspergillus flavus* at 25 °C for 48 h, for *Candida albicans* at 30 °C for 48 h and for all bacteria at 35 °C for 24 h). The antimicrobial potential by all substances (20 mg/mL) in DMSO was determined, and pure DMSO (afforded no microbial inhibition) represented the negative control. Blank discs (8.0 mm) obtained from Schleicher & Schuell (Spain) were impregnated with ten microliters from each compound solution. After putting the discs on the agar surfaces, microbial inhibitions occurred in the areas around the discs. The inhibition area diameters (synonym, the inhibition zones) were estimated, considering the National Committee for Clinical Laboratory Standards.

2.4. Cytotoxic Activity Assay in Cancer and Normal Cells

Breast MCF-7 and normal BHK cells were provided from the American Type Culture Collection. The anti-proliferative activities by HL and its Ni(II) complex, as well as Sigma-Aldrich purchased doxorubicin (0–0.1 mg/mL in DMSO), were thrice determined as follows [64]. Initially, the cells (4000 cells/well) were incubated in fresh medium (200 μ L) at 37 °C in less than 5% of CO₂. After 24 h, each compound solution was added to a cell plate. Following incubation for 48 h, fixing the cultures with trichloroacetic acid (50 μ L, 50%) at 4 °C and washing with distilled water, fifty microliters of sulforhodamine B solution (0.4% dissolved in acetic acid (1%)) were added in the dark at ambient atmosphere, and the cultures were rewashed with acetic acid (1%). After air drying, TRIS base (10 mM, pH = 10.5, 200 μ L) was put in each well to solubilize the dye, and the optical density was investigated at 570 nm using an ELISA microtiter plate reader. Plates with pure DMSO replacing the compound solution are considered with 100% cell viability.

2.5. Effects on Drought-Sensitive and Drought-Resistive Wheat Cultivars

Grains of two wheat cultivars (Gim-7 (drought-sensitive) and Sids-1 (drought-resistive)) were incorporated in the experiment. The grains were soaked for 12 h in the ligand/complex solution (1000 ppm), and grains soaked in pure distilled water acted as control. After soaking, the grains were transferred into 40 \times 30 cm iron pots containing sandy-sterilized soil of 5 cm depth. Half the grains from each type were irrigated at normal field capacity (30%), while the remaining grains experienced drought conditions achieved using polyethylene glycol (PEG, 15%). For seven days, water was added daily to maintain the soil at the field capacity and, after day two, the germination was daily investigated. Germinated seeds are those with ≥ 1 mm protruded plumule through the seed coat [65]. After day seven, the total number of germinated seeds was determined. The effect of the ligand and its complex on the seed germination was investigated by calculating the germination percentages and the germination velocity coefficients [66].

2.6. Statistical Analysis

One-way ANOVA was applied to assess the variations in the different biological treatments. Analysis of variance (ANOVA) was carried out using a general one-way model using SPSS v.25.

3. Results and Discussion

3.1. Formation of the Nickel Complex

The ligand (Figure 1) was prepared in an almost quantitative yield via mixing equivalents of salicylaldehyde and 3,4-dimethylaniline in ethanol [62]. This Schiff base was characterized by CHN analyses and FT-IR and ^1H - and ^{13}C -NMR spectroscopy, and all spectral data were typical to those reported [62]. The salicylaldehyde ligands are generally known to bind in a bidentate monobasic chelation mode via their imine N and deprotonated phenol O atoms [67]. In ethanol, mixing **HL** with nickel(II) chloride hexahydrate (2:1 molar ratio) resulted in instant green precipitation that was crystallized using dichloromethane (yield = 91%) as air stable and non-hygroscopic crystals. As a DMF solution (1×10^{-3} M), the complex electrical conductivity ($12.14 \Omega^{-1}\text{cm}^2\text{mol}^{-1}$) indicated its molecular character [68].

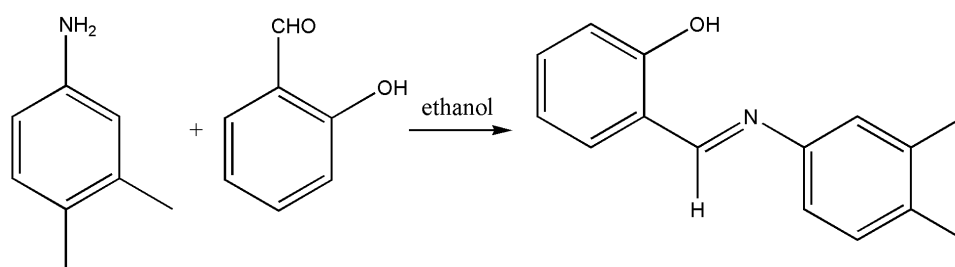


Figure 1. Preparation strategy of the ligand.

Spectroscopic (FT-IR and ultraviolet-visible light) measurements were performed for the complex and its ligand to elucidate the functional groups, as well as the assignments for the electronic transitions in these compounds. The IR spectrum of the nickel complex, when compared with that of the unbound ligand, strongly indicated the metal coordination. First, the stretching vibration due to $\nu(\text{C}=\text{N})$ at 1607 cm^{-1} in the complex spectrum is seen at a higher wavenumber of 1635 cm^{-1} for the unbound ligand, as the Ni—N coordination weakens the azonmethine bond [69]. The ligand displayed a broad transition at 3262 cm^{-1} assignable to the O—H bond vibration; this band disappeared in the complex spectrum suggesting deprotonation of this group in the complex [69]. New distinct bands are seen in the complex spectrum at 573 and 452 cm^{-1} due to vibrations in the Ni—O and Ni—N bonds, respectively [69]. The electronic spectra of **HL** and its Ni(II) complex were measured in DMSO. For the ligand, only one peak is seen at 345 nm due to $n-\pi^*$ transition in the Schiff base. For the Ni(II) complex, this intraligand band slightly moved to 340 nm and another band appeared at 607 nm , due to the $^3\text{A}_{2g}(\text{F}) \rightarrow ^3\text{T}_{1g}(\text{F})$ transition [68]. In fact, octahedral Ni(II) compounds should afford two other d-d transitional bands [$^3\text{A}_{2g}(\text{F}) \rightarrow ^3\text{T}_{1g}(\text{P})$ and $^3\text{A}_{2g}(\text{F}) \rightarrow ^3\text{T}_{2g}(\text{F})$], but these were not detected due to tailing of the intraligand band for the first transition and the expected appearance at a long wavelength $\approx 950 \text{ nm}$ for the latter one [69].

3.2. X-ray Diffraction Analysis

Figures 2 and 3 present the crystal structure and packing scheme of the nickel complex, respectively, while the complex most relevant bond lengths and angles are listed in Table 2. Generally, the complex is trinuclear with three almost linear nickel atoms ($\text{Ni1—Ni2—Ni1}^i = 179.54^\circ$). Indeed, the mononuclear Ni(II)-salicylaldehydes are more predominant in the literature, but three isostructural trinuclear nickel complexes, with ligands derived from salicylaldehyde and 1-bromoaniline, 1-methylaniline and 1-methoxyaniline, displaying Ni1—Ni2—Ni1ⁱ angles = 178.71 – 179.72° , were recently reported [70].

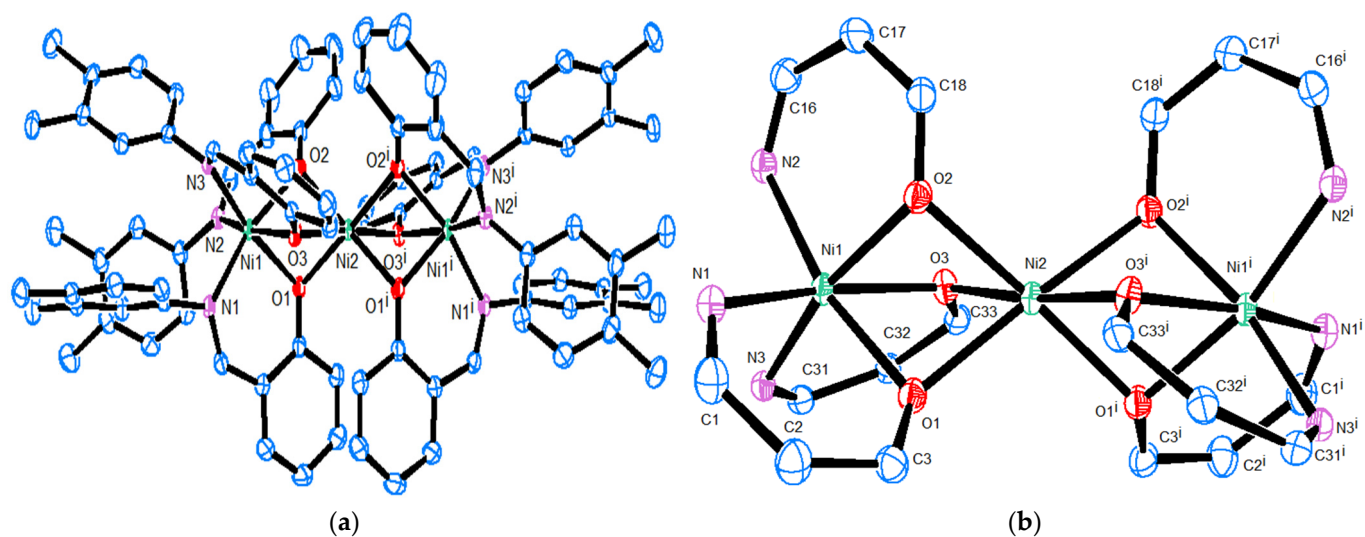


Figure 2. Representation of the Ni(II) complex molecular structure with (a) all H-atoms and solvent molecules removed for clarity and (b) only chelate rings showing the coordination mode with nickel.

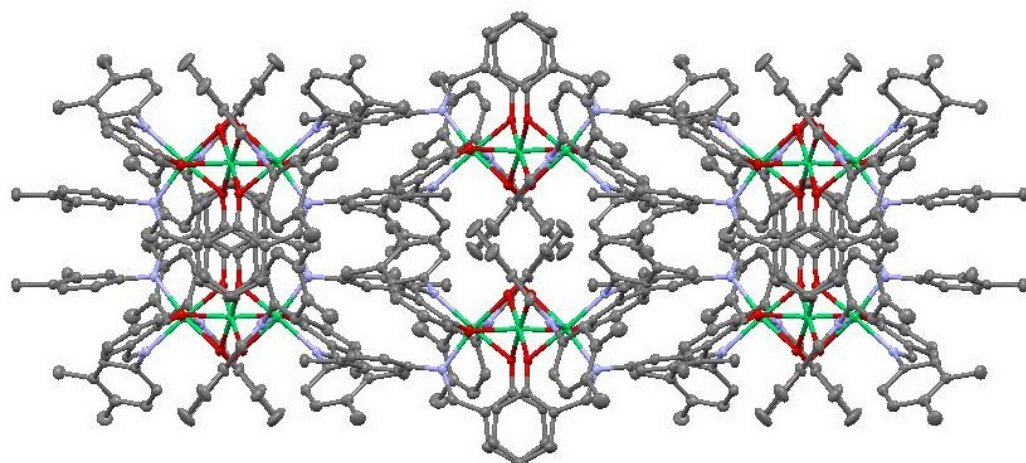


Figure 3. Packing of the complex along c-axis.

This centrosymmetric complex crystallized in the monoclinic space group $C 2/c$ and its asymmetric unit is represented by half of the complex molecule. In this structure, the octahedral coordination environment exists around each of the three nickel atoms. This environment for the terminal cations is identical with three N(azomethine) and three O(phenol) atoms (N1, N2, N3, O1, O2 and O3), as expected for the coordination with the salicylaldehyde Schiff bases [70]. However, only the same oxygen atoms that bind the terminal cations connect with the central nickel atom to build its coordination sphere. Further, disordered molecules of the crystallization solvent, dichloromethane, occupied some positions in the crystal lattice. The chelation in this complex resulted in a Ni–Ni distance of 2.8266 Å between the central and terminal nickel cations, and Ni–O and Ni–N distances in agreement with literature [70] that reported Ni–Ni, Ni–O and Ni–N distances of 2.8116(6)–2.8248(2), 2.037(3)–2.0560(10) and 2.070(3)–2.099(3) Å, respectively.

Table 2. Selected bond lengths (Å) and angles (°) in the nickel complex.

Atoms	Distance (Å)	Atoms	Angle (°)	Atoms	Angle (°)
N1—Ni1	2.081 (1)	C3—O1—Ni1	129.6 (1)	O1—Ni2—O2	77.46
N2—Ni1	2.080 (2)	Ni2—O1—C3	128.82	O2—Ni2—O2 ⁱ	99.16
N3—Ni1	2.090 (1)	Ni2—O1—Ni1	86.14	O1—Ni2—O1 ⁱ	106.16
Ni1—O1	2.056 (1)	Ni2—O2—C18	133.25	O1—Ni2—O2 ⁱ	174.90
Ni1—O2	2.051 (1)	Ni2—O2—Ni1	86.76	O1—Ni2—O3 ⁱ	99.21
Ni1—O3	2.041 (1)	N1—Ni1—N2	97.53 (6)	O2—Ni2—O3	77.91
Ni2—O1	2.083	N1—Ni1—N3	95.38 (6)	O3—Ni2—O3 ⁱ	174.68
Ni2—O2	2.065	N2—Ni1—O1	93.45(5)	O2—Ni2—O3 ⁱ	105.65
Ni2—O3	2.040	N3—Ni1—O1	166.44 (5)	O1—Ni2—O3	77.54
C3—O1	1.306 (2)	C1—N1—Ni1	124.2 (1)	N3—Ni1—O3	88.90 (5)
C18—O2	1.306 (2)	C8—N1—Ni1	122.3 (1)	Ni2—O3—C33	131.56
C33—O3	1.314 (2)	C23—N2—Ni1	122.4 (1)	C18—O2—Ni1	130.2 (1)
C1—N1	1.285 (2)	C31—N3—Ni1	123.5 (1)	N2—Ni1—N3	98.42 (6)
C8—N1	1.442 (2)	C38—N3—Ni1	121.7 (1)	N1—Ni1—O3	94.16 (5)
C16—N2	1.290 (2)	N1—Ni1—O1	89.51 (5)	N1—Ni1—O2	166.74 (5)
C23—N2	1.434 (3)	C16—N2—Ni1	123.8 (1)	N3—Ni1—O2	95.29 (5)
C31—N3	1.288 (2)	Ni2—O3—Ni1	87.70	O1 ⁱ —Ni1—O3	78.12 (5)
C38—N3	1.439 (3)	C33—O3—Ni1	130.4 (1)	N2—Ni1—O3	165.54 (6)
		O1 ⁱ —Ni1—O2	78.38 (5)	N2—Ni1—O2	88.65 (5)

Strong chelation for all nickel atoms exists in the structure. The terminal nickel cations are chelated in three six-membered rings with torsion angles of 81.081°, 83.753° and 88.681° between the rings' planes. Each chelate ring has a torsion angle of 5.814° with the fused benzene ring, while twisting in each ligand molecule is indicated due to a torsion angle of 64.278° between its phenyl rings. In addition to extensive network of hydrogen bonds with carbon atoms connecting the complex molecules, the crystallization solvent contributes to this bonding. But no accurate metrics can be calculated for these bonds due to the disorder in the solvent location.

3.3. Microbial Inhibition Data

Figure 4 presents the antibacterial action of **HL** and its nickel complex as well as ampicillin (20 mg/mL in DMSO), against *Bacillus subtilis*, *Staphylococcus aureus*, *Escherichia coli* and *Pseudomonas aeruginosa* strains, investigated through the Kirby–Bauer disc diffusion method [63].

Here, ampicillin generated inhibition diameters with 26, 21, 25 and 26 mm against these strains, respectively. These are actually greater inhibitions compared to the complex induced inhibition diameters (12, 13, 10 and 11 mm against *Bacillus subtilis*, *Staphylococcus aureus*, *Escherichia coli* and *Pseudomonas aeruginosa*, respectively). But, interestingly, great enhancement in the ligand activity occurred after its coordination, as the ligand only inhibited the *Staphylococcus aureus* bacteria with 10 mm. Similarly to the compounds' action on bacteria, the ligands did not show any activity on the *Aspergillus flavus* and *Candida albicans* fungal strains (Figure 5), but the standard (amphotericin B) induced activities with 17 and 21 mm against these fungi, respectively. On the other hand, the coordination with nickel enhanced the ligand activity against *Candida albicans* to 13 mm.

Indeed, the enhancement in the antimicrobial activity upon complexation can be explained by Tweedy's chelation theory [71]. The ligand bioactivity enhancement after coordination makes the metal complexes prescribed at lower dosages similar to long-acting drugs, due to their slow dissociation in the cells [72,73].

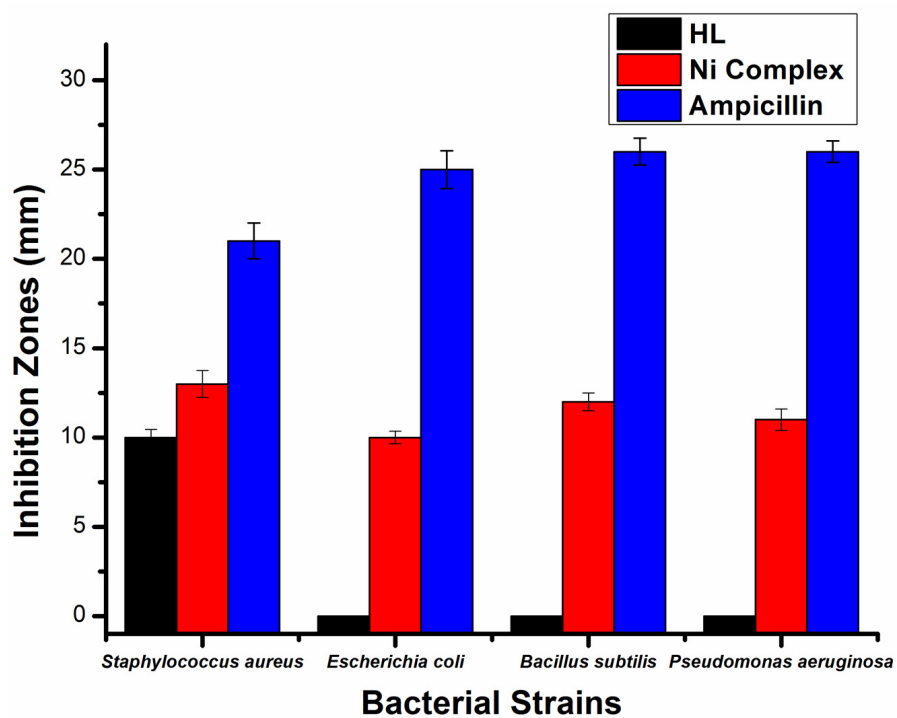


Figure 4. Bioactivity data obtained by the salicylalimine ligand and its nickel complex (20 mg/mL) against *S. aureus*, *B. subtilis*, *S. aureus* and *E. coli*.

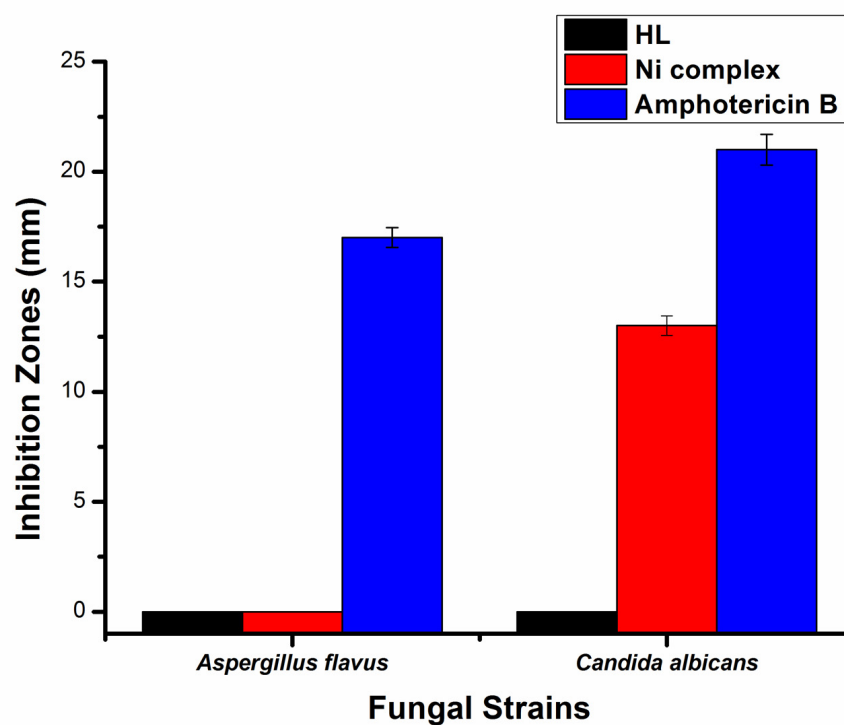


Figure 5. A plot displaying the correlation between HL and its complex (20 mg/mL) and the induced inhibition in *A. flavus* and *C. albicans* strains.

3.4. Cytotoxic Activity Data

Being regarded as the cancer type of the most crucial incidence rate for women, we studied the effect of our compounds on model breast cancer cells (MCF-7) [74]. Moreover, we preferred to apply in vitro procedures for the sulforhodamine B method (Figure 6) than the MTT (3-(4,5-dimethylthiazol-2-yl)-2,5-diphenyltetrazolium bromide) method, as the latter method suffers a probable reduction in MTT even if the cells are not affected [64].

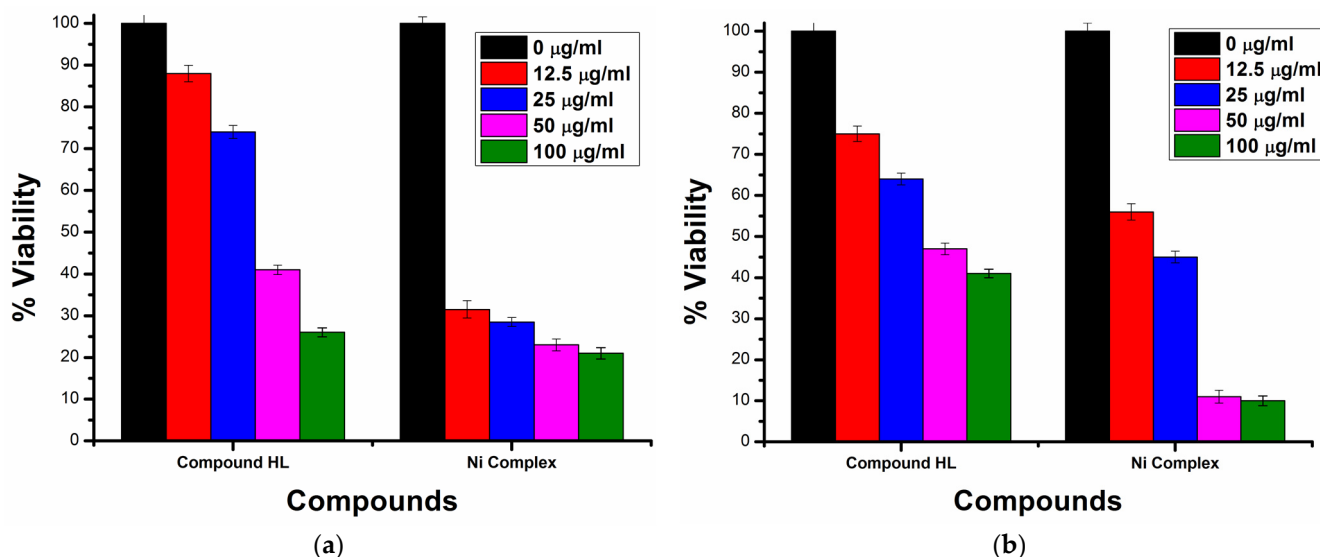


Figure 6. Cytotoxicity data of HL and the nickel complex against (a) MCF-7 cancer and (b) BHK normal cells.

Applying various concentrations (0–100 µg/mL) of both HL and its complex on MCF-7 cells showed very weak ligand cytotoxicity with an IC_{50} value = 195.5 µM. But nickel, when coordinated, much enhanced this activity to an IC_{50} value = 5.44 µM. In the literature [69], we found five mononuclear nickel salicylaldehyde complexes with IC_{50} values of 65.3–236.28 µM, compared to IC_{50} = 17.24–175.45 µM for their ligands. The greater activity of our complex compared to those in literature may be due to its trinuclear nature, which means, compared to a mononuclear complex, our complex triples the concentrations of both Ni(II) ions and ligands after its dissociation in cells.

To obtain a clearer picture of the anti-cancer activity of this complex, we also studied its action in normal BHK cells compared to a standard (doxorubicin). Indeed, the ligand was also almost inactive in the BHK cells (IC_{50} = 199.9 µM), but the complex showed great toxicity (IC_{50} = 11.61 µM) in them. This complex toxicity is lower than that activity against the breast cells. But doxorubicin acted with IC_{50} values of 9.66 and 36.42 µM in the MCF-7 and BHK cells, respectively, concluding that the complex is more active than the standard in both cell types.

3.5. Effects on Drought-Sensitive and Drought-Resistive Wheat Cultivars

Here, we detected how the ligand and its nickel complex affected the germination process of drought-sensitive (Gim 7) and drought-resistive (Sids 1) wheat cultivars under normal irrigation and drought conditions. To do so, we soaked the wheat grains in 1000 ppm solutions of the compounds prior to determining the percentages of germination and the respective velocity coefficients due to the exposure to our compounds (Figure 7).

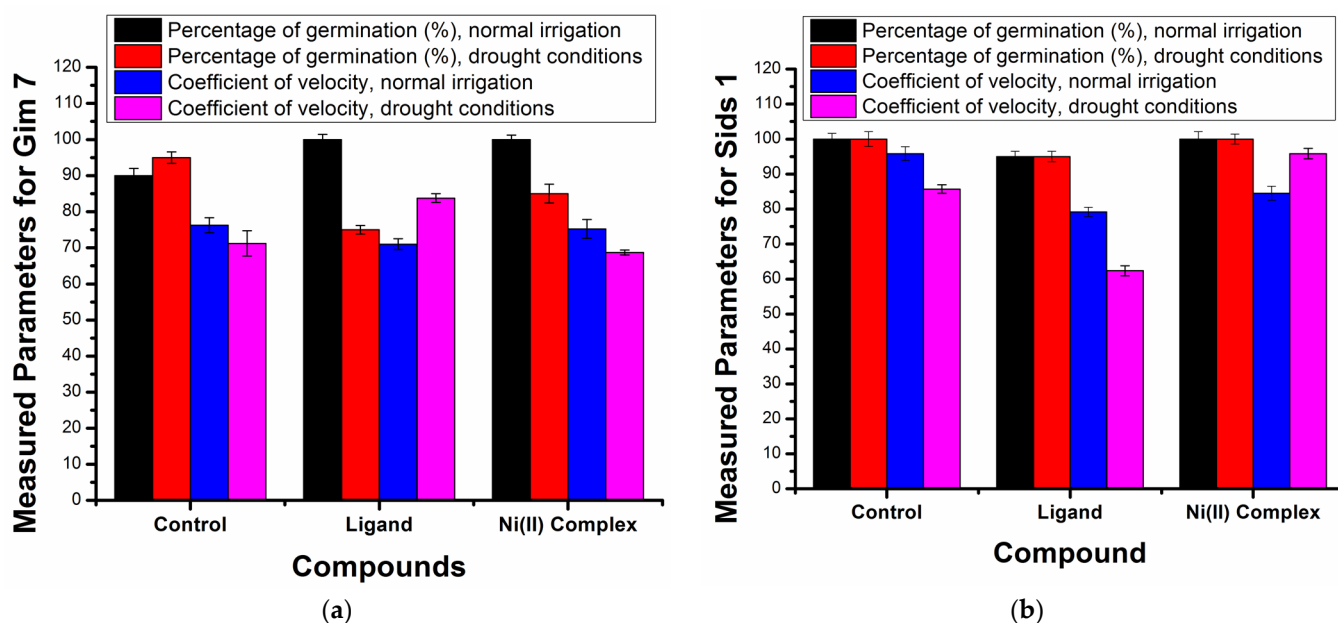


Figure 7. Germination percentage and velocity coefficient data of two wheat cultivars, Gim 7 (a) and Sids 1 (b), under normal irrigation and drought conditions.

For the drought-sensitive grains (Gim 7), under normal irrigation, we observed that both the ligand and its complex afforded 100% germination percentages higher than the control (90%). This reflects the importance of both the organic molecule as well as the Ni(II) ions for the Gim 7 germination. However, under drought, Gim 7 germination followed a different order (control (95%) > nickel complex (85%) > ligand (75%)). This order suggests improved germination by the nickel complex, due to probable synergism between the resulting nickel ions and the organic ligand after the complex dissociation. On the other hand, for Sids 1 under both normal irrigation and drought conditions, we detected the same results as follows: both the control and the nickel complex afforded 100% germination percentage, while the ligand lowered this percentage to 95%. Consistent with previous studies [75], our results suggest that the effects of the ligand and its nickel complex on the germination process of wheat cultivars can vary, depending on the cultivar type and the environmental conditions. In addition, the mechanisms underlying the observed effects may involve interactions between the ligand, metal ion and plant cells [76].

It should be noted that, for both cultivars under normal irrigation, the control pots had an accelerated germination process compared to the nickel complex which, in turn, afforded faster germination than the ligand (the control, nickel complex and ligand afforded velocity coefficients of 76.3, 75.2 and 71.0 (for Gim 7) and of 95.8, 84.5 and 79.2 (for Sids 1), respectively). However, under drought conditions, a reversed order for Gim 7 and Sids 1 was detected (for Gim 7, velocity coefficients of 83.8 (ligand) > 71.2 (control) > 68.7 (nickel complex) and for Sids 1, velocity coefficients of 95.8 (nickel complex) > 85.7 (control) > 62.3 (ligand) were detected). These varied velocity coefficients suggest that the complexes affect different stages in the germination process and plant development [77]. Therefore, this nickel complex may have conditional potential to improve the germination of wheat cultivars, but understanding the mechanisms underlying the observed effects and optimizing the use of this complex for agricultural applications need further studies.

4. Conclusions

This research showed the synthesis of a trinuclear nickel complex with a bidentate salicylaldimine ligand. This complex is centrosymmetric, with two terminal nickel atoms coordinated with N_3O_3 coordination systems and a central atom coordinated with six oxygen atoms. The complex revealed greater antibacterial and antifungal activities than the ligand,

but not exceeding the standards. More interesting is that this complex is significantly cytotoxic to breast cancer cells (more toxic than the standard), but also induced high toxicity in normal cells. For drought-sensitive wheat under normal irrigation, both the ligand and its complex afforded 100% germination, but under drought, the higher germination percentage was recorded for the control. For drought-resistive wheat, the control and the nickel complex afforded 100% germination percentage under normal irrigation and drought conditions.

Author Contributions: Conceptualization, A.A., A.B.M.I., S.A.E. and S.M.A.; methodology, E.S.W., A.A., A.B.M.I., P.M. and S.M.A.; investigation, E.S.W., A.A., A.B.M.I. and S.M.A.; writing—original draft preparation, A.B.M.I.; writing—review and editing, E.S.W., A.A., A.B.M.I., S.A.E., P.M. and S.M.A.; visualization, A.B.M.I.; supervision, A.B.M.I., S.A.E. and S.M.A. All authors have read and agreed to the published version of the manuscript.

Funding: This research received no external funding.

Data Availability Statement: Crystallographic supplementary data can be received at no charge from the website <https://www.ccdc.cam.ac.uk/structures/> (Deposition number: CCDC 2269814).

Acknowledgments: The authors thank Ivana Císarová (Charles University, Czech Republic) for her help in collecting the crystallographic data and solving the crystal structure of the complex.

Conflicts of Interest: The authors declare no conflict of interest.

References

1. Tidwell, T.T. Hugo (Ugo) Schiff, Schiff bases, and a century of beta-lactam synthesis. *Angew. Chem. Int. Ed.* **2008**, *47*, 1016–1020. [[CrossRef](#)] [[PubMed](#)]
2. Krishnamoorthy, P.; Sathyadevi, P.; Muthiah, P.T.; Dharmaraj, N. Nickel and cobalt complexes of benzoic acid (2-hydroxybenzylidene)-hydrazide ligand: Synthesis, structure and comparative *in vitro* evaluations of biological perspectives. *RSC Adv.* **2012**, *2*, 12190–12203. [[CrossRef](#)]
3. Yang, W.; Liu, H.; Du, D. Efficient in situ three-component formation of chiral oxazoline-Schiff base copper(ii) complexes: Towards combinatorial library of chiral catalysts for asymmetric Henry reaction. *Org. Biomol. Chem.* **2010**, *8*, 2956–2960. [[CrossRef](#)] [[PubMed](#)]
4. Sano, T.; Nishio, Y.; Hamada, Y.; Takahashi, H.; Usuki, T.; Shibata, K. Design of conjugated molecular materials for optoelectronics. *J. Mater. Chem.* **2000**, *10*, 157–161. [[CrossRef](#)]
5. Lee, S.A.; You, G.R.; Choi, Y.W.; Jo, H.Y.; Kim, A.R.; Noh, I.; Kim, S.J.; Kim, Y.; Kim, C. A new multifunctional Schiff base as a fluorescence sensor for Al³⁺ and a colorimetric sensor for CN⁻ in aqueous media: An application to bioimaging. *Dalton Trans.* **2014**, *43*, 6650–6659. [[CrossRef](#)]
6. Nayar, C.R.; Ravikumar, R. Review: Second order nonlinearities of Schiff bases derived from salicylaldehyde and their metal complexes. *J. Coord. Chem.* **2014**, *67*, 1–16. [[CrossRef](#)]
7. Li, S.; Chen, S.; Lei, S.; Ma, H.; Yu, R.; Liu, D. Investigation on some Schiff bases as HCl corrosion inhibitors for copper. *Corros. Sci.* **1999**, *41*, 1273–1287. [[CrossRef](#)]
8. Al Zoubi, W.; Al Mohanna, N. Membrane sensors based on Schiff bases as chelating ionophores—a review. *Spectrochim. Acta A Mol. Biomol. Spectrosc.* **2014**, *132*, 854–870. [[CrossRef](#)]
9. Jeevadason, A.W.; Murugavel, K.K.; Neelakantan, M.A. Review on Schiff bases and their metal complexes as organic photovoltaic materials. *Renew. Sustain. Energy Rev.* **2014**, *36*, 220–227. [[CrossRef](#)]
10. Nakayama, A.; Hiromura, M.; Adachi, Y.; Sakurai, H. Molecular mechanism of antidiabetic zinc-allixin complexes: Regulations of glucose utilization and lipid metabolism. *J. Biol. Inorg. Chem.* **2008**, *13*, 675–684. [[CrossRef](#)]
11. Sakurai, H.; Yoshikawa, Y.; Yasui, H. Current state for the development of metallopharmaceuticals and anti-diabetic metal complexes. *Chem. Soc. Rev.* **2008**, *37*, 2383–2392. [[CrossRef](#)] [[PubMed](#)]
12. Panneerselvam, P.; Nair, R.R.; Vijayalakshmi, G.; Subramanian, E.H.; Sridhar, S.K. Synthesis of Schiff bases of 4-(4-aminophenyl)-morpholine as potential antimicrobial agents. *Eur. J. Med. Chem.* **2005**, *40*, 225–229. [[CrossRef](#)]
13. Ren, S.; Wang, R.; Komatsu, K.; Bonaz-Krause, P.; Zyrianov, Y.; McKenna, C.E.; Csipke, C.; Tokes, Z.A.; Lien, E.J. Synthesis, biological evaluation, and quantitative structure–activity relationship analysis of new Schiff bases of hydroxysemicarbazide as potential antitumor agents. *J. Med. Chem.* **2002**, *45*, 410–419. [[CrossRef](#)] [[PubMed](#)]
14. Mendu, P.; Kumari, C.G.; Ragi, R. Synthesis, characterization, DNA binding, DNA cleavage and antimicrobial studies of Schiff base ligand and its metal complexes. *J. Fluoresc.* **2015**, *25*, 369–378. [[CrossRef](#)]
15. de Fátima, A.; de Paula Pereira, C.; Olímpio, C.R.S.D.G.; de Freitas Oliveira, B.G.; Franco, L.L.; da Silva, P.H.C. Schiff bases and their metal complexes as urease inhibitors—A brief review. *J. Adv. Res.* **2018**, *13*, 113–126. [[CrossRef](#)] [[PubMed](#)]

16. Naskar, B.; Modak, R.; Sikdar, J.; Maiti, D.K.; Banik, A.; Dangar, T.K.; Mukhopadhyay, S.; Mandal, D.; Goswami, S. A simple Schiff base molecular logic gate for detection of Zn²⁺ in water and its bio-imaging application in plant system. *J. Photochem. Photobiol. Chem.* **2016**, *321*, 99–109. [[CrossRef](#)]
17. Garnovski, A.D.; Vasilchenko, I.S. Rational design of metal coordination compounds with azomethine ligands. *Russ. Chem. Rev.* **2002**, *71*, 943–968. [[CrossRef](#)]
18. Das, P.; Linert, W. Schiff base-derived homogeneous and heterogeneous palladium catalysts for the Suzuki–Miyaura reaction. *Coord. Chem. Rev.* **2016**, *311*, 1–23. [[CrossRef](#)]
19. Opstal, T.; Verpoort, F. Synthesis of highly active ruthenium indenylidene complexes for atom-transfer radical polymerization and ring-opening-metathesis polymerization. *Angew. Chem. Int. Ed.* **2003**, *42*, 2876–2879. [[CrossRef](#)]
20. Yoon, T.P.; Jacobsen, E.N. Privileged chiral catalysts. *Science* **2003**, *299*, 1691–1693. [[CrossRef](#)]
21. Nejati, K.; Rezvani, Z.; Massoumi, B. Syntheses and investigation of thermal properties of copper complexes with azo-containing Schiff-base dyes. *Dyes Pigm.* **2007**, *75*, 653–657. [[CrossRef](#)]
22. Tantar, G.; Dorneanu, V.; Stan, M. Schiff bis bases: Analytical reagents. II. Spectrophotometric determination of manganese from pharmaceutical forms. *J. Pharm. Biomed. Anal.* **2002**, *27*, 827–832. [[CrossRef](#)]
23. El-Bindary, A.A.; El-Sonbati, A.Z.; Diab, M.A.; Ghoneim, M.M.; Serag, L.S. Polymeric complexes—LXII. Coordination chemistry of supramolecular Schiff base polymer complexes—A review. *J. Mol. Liq.* **2016**, *216*, 318–329. [[CrossRef](#)]
24. Zhang, J.; Xu, L.; Wong, W.-Y. Energy materials based on metal Schiff base complexes. *Coord. Chem. Rev.* **2018**, *355*, 180–198. [[CrossRef](#)]
25. Hothi, H.S.; Makkar, A.; Sharma, J.R.; Manrao, M.R. Synthesis and antifungal potential of Co(II) complexes of 1-(2'-hydroxyphenyl) ethylideneanilines. *Eur. J. Med. Chem.* **2006**, *41*, 253–255. [[CrossRef](#)]
26. Sreedaran, S.; Bharathi, K.S.; Kalilur-Rahiman, A.; Rajesh, K.; Nirmala, G.; Jagadish, L.; Kaviyaran, V.; Narayana, V. Synthesis, electrochemical, catalytic and antimicrobial activities of novel unsymmetrical macrocyclic dicompartmental binuclear nickel(II) complexes. *Polyhedron* **2008**, *27*, 1867–1874. [[CrossRef](#)]
27. Li, Z.; Yan, H.; Chang, G.; Hong, M.; Dou, J.; Niu, M. Cu(II), Ni(II) complexes derived from chiral Schiff-base ligands: Synthesis, characterization, cytotoxicity, protein and DNA-binding properties. *J. Photochem. Photobiol. B* **2016**, *163*, 403–412. [[CrossRef](#)] [[PubMed](#)]
28. Dhara, K.; Roy, P.; Ratha, J.; Manassero, M.; Banerjee, P. Synthesis, crystal structure, magnetic property and DNA cleavage activity of a new terephthalate-bridged tetranuclear copper(II) complex. *Polyhedron* **2007**, *26*, 4509–4517. [[CrossRef](#)]
29. Mondal, S.; Chakraborty, M.; Mondal, A.; Pakhira, B.; Blake, A.J.; Sinn, E.; Chattopadhyay, S.K. Cu(ii) complexes of a tridentate N,N,O-donor Schiff base of pyridoxal: Synthesis, X-ray structures, DNA-binding properties and catecholase activity. *New J. Chem.* **2018**, *42*, 9588–9597. [[CrossRef](#)]
30. Baumeister, J.E.; Reinig, K.M.; Barnes, C.L.; Kelley, S.P.; Jurisson, S.S. Technetium and rhenium Schiff base compounds for nuclear medicine: Syntheses of rhenium analogues to ^{99m}Tc-furifosmin. *Inorg. Chem.* **2018**, *57*, 12920–12933. [[CrossRef](#)]
31. Golbedaghi, R.; Fausto, R. Coordination aspects in Schiff bases cocrystals. *Polyhedron* **2018**, *155*, 1–12. [[CrossRef](#)]
32. Chowdhury, T.; Bera, K.; Samanta, D.; Dolui, S.; Maity, S.; Maiti, N.C.; Ghosh, P.K.; Das, D. Unveiling the binding interaction of zinc (II) complexes of homologous Schiff-base ligands on the surface of BSA protein: A combined experimental and theoretical approach. *Appl. Organomet. Chem.* **2020**, *34*, e5556. [[CrossRef](#)]
33. Mondal, S.S.; Jaiswal, N.; Bera, P.S.; Tiwari, R.K.; Behera, J.N.; Chanda, N.; Ghosal, S.; Saha, T.K. Cu(II) and Co(II/III) complexes of N,O-chelated Schiff base ligands: DNA interaction, protein binding, cytotoxicity, cell death mechanism and reactive oxygen species generation studies. *Appl. Organomet. Chem.* **2021**, *35*, e6026. [[CrossRef](#)]
34. Adsule, S.; Barve, V.; Chen, D.; Ahmed, F.; Dou, Q.P.; Padhye, S.; Sarkar, F.H. Novel Schiff base copper complexes of quinoline-2 carboxaldehyde as proteasome inhibitors in human prostate cancer cells. *J. Med. Chem.* **2006**, *49*, 7242–7246. [[CrossRef](#)]
35. Ibrahim, A.B.M.; Mahmoud, G.A.-E. Chemical- vs sonochemical-assisted synthesis of ZnO nanoparticles from a new zinc complex for improvement of carotene biosynthesis from *Rhodotorula toruloides* MH023518. *Appl. Organomet. Chem.* **2021**, *35*, e6086. [[CrossRef](#)]
36. Ibrahim, A.B.M.; Mahmoud, G.A.-E.; Meurer, F.; Bodensteiner, M. Preparation and crystallographic studies of a new mercuric salicylaldimine complex for fabrication of microscaled and nanoscaled mercuric sulfide as antimicrobial agents against human pathogenic yeasts and filamentous fungi. *Appl. Organomet. Chem.* **2021**, *35*, e6134. [[CrossRef](#)]
37. Kasumov, V.T.; Köksal, F. Synthesis, ESR, UV-Visible and reactivity studies of new bis(N-dimethoxyaniline-3,5-^tBu₂-salicylaldiminato)copper(II) complexes. *Spectrochim. Acta A Mol. Biomol. Spectrosc.* **2012**, *98*, 207–214. [[CrossRef](#)] [[PubMed](#)]
38. Kasumov, V.T.; Köksal, F.; Sezer, A. Synthesis, spectroscopic and redox properties of a novel series of copper(II) complexes of N-alkyl-3,5-^tBu₂-salicylaldimines. Generation of the directly coordinated Cu(II)-phenoxy radical complexes. *Polyhedron* **2005**, *24*, 1203–1211. [[CrossRef](#)]
39. Venkataramanan, N.S.; Kuppuraj, G.; Rajagopal, S. Metal-salen complexes as efficient catalysts for the oxygenation of heteroatom containing organic compounds-synthetic and mechanistic aspects. *Coord. Chem. Rev.* **2005**, *249*, 1249–1268. [[CrossRef](#)]
40. Katsuki, T. Unique asymmetric catalysis of *cis*- β metal complexes of salen and its related Schiff-base ligands. *Chem. Soc. Rev.* **2004**, *33*, 437–444. [[CrossRef](#)]
41. Yiang, X.; Jones, R.A. Anion dependent self-assembly of “Tetra-Decker” and “Triple-Decker” luminescent Tb(III) salen complexes. *J. Am. Chem. Soc.* **2005**, *127*, 7686–7687. [[CrossRef](#)] [[PubMed](#)]

42. Campell, N.H.; Abd Karim, N.H.; Parkinson, G.N.; Gunaratnam, M.; Petrucci, V.; Todd, A.K.; Vilar, R.; Neidle, S. Molecular basis of structure–activity relationships between salphen metal complexes and human telomeric DNA quadruplexes. *J. Med. Chem.* **2012**, *55*, 209–222. [[CrossRef](#)]
43. Prabhakar, M.; Zacharias, P.S.; Das, S.K. Self-assembly of a fluorescent chiral zinc(II) complex that leads to supramolecular helices. *Inorg. Chem.* **2005**, *44*, 2585–2587. [[CrossRef](#)]
44. Teixeira, M.F.S.; Dockal, E.R.; Cavalheiro, E.T.G. Sensor for cysteine based on oxovanadium(IV) complex of Salen modified carbon paste electrode. *Sens. Actuat. B Chem.* **2005**, *106*, 619–625. [[CrossRef](#)]
45. Wang, C.M.; Friedrich, S.; Younkin, T.R.; Li, R.T.; Grubbs, R.H.; Bansleben, D.A.; Day, M.W. Neutral nickel(II)-based catalysts for ethylene polymerization. *Organometallics* **1998**, *17*, 3149–3151. [[CrossRef](#)]
46. Younkin, T.R.; Connor, E.F.; Henderson, J.I.; Friedrich, S.K.; Grubbs, R.H.; Bansleben, D.A. Neutral, single-component nickel(II) polyolefin catalysts that tolerate heteroatoms. *Science* **2000**, *287*, 460–462. [[CrossRef](#)]
47. Dhara, P.K.; Sarkar, S.; Drew, M.G.B.; Nethaji, M.; Chattopadhyay, P. Nickel(II) complexes of tetradentate NSNO pyridylthioazophenol ligands: Synthesis, characterization and crystal structure. *Polyhedron* **2008**, *27*, 2447–2451. [[CrossRef](#)]
48. Claudel, M.; Schwarte, J.V.; Fromm, K.M. New antimicrobial strategies based on metal complexes. *Chemistry* **2020**, *2*, 849–899. [[CrossRef](#)]
49. Bharati, P.; Bharti, A.; Bharty, M.K.; Maiti, B.; Butcher, R.J.; Singh, N.K. Square planar Ni(II) complexes of pyridine-4-carbonylhydrazine carbodithioate, 1-phenyl-3-pyridin-2-yl-isothiourea and 4-(2-methoxyphenyl)piperazine-1-carbodithioate involving N–S bonding: An approach to DFT calculation and thermal studies. *Polyhedron* **2013**, *63*, 156–166. [[CrossRef](#)]
50. Bartha, R.; Ordal, E.J. Nickel-dependent chemolithotrophic growth of two hydrogenomonas strains. *J. Bacteriol.* **1965**, *89*, 1015–1019. [[CrossRef](#)] [[PubMed](#)]
51. Hausinger, R.P. Nickel utilization by microorganisms. *Microbiol. Rev.* **1987**, *51*, 22–42. [[CrossRef](#)]
52. Fierros-Romero, G.; Wrosek-Cabrera, J.A.; Gomez-Ramirez, M.; Pless, R.C.; Rivas-Castillo, A.M.; Rojas-Avelizapa, N.G. Expression changes in metal-resistance genes in *Microbacterium liquefaciens* under nickel and vanadium exposure. *Curr. Microbiol.* **2017**, *74*, 840–847. [[CrossRef](#)]
53. Kumar, S.; Trivedi, A.V. A review on role of nickel in the biological system. *Int. J. Curr. Microbiol. Appl. Sci.* **2016**, *5*, 719–727. [[CrossRef](#)]
54. Saad, E.A.; Hassanien, M.M.; Ellban, F.W. Nickel(II) diacetyl monoxime-2-pyridyl hydrazone complex can inhibit Ehrlich solid tumor growth in mice: A potential new antitumor drug. *Biochem. Biophys. Res. Commun.* **2017**, *484*, 579–585. [[CrossRef](#)]
55. Gilbert, J.G.; Addison, A.W.; Nazarenko, A.Y.; Butcher, R.J. Copper(II) complexes of new unsymmetrical NSN thioether ligands. *Inorganica Chim. Acta* **2001**, *324*, 123–130. [[CrossRef](#)]
56. Zhu, L.-N.; Kong, D.-M.; Li, X.-Z.; Wang, G.-Y.; Jin, Y.-W. DNA cleavage activities of tetraazamacrocyclic oxamido nickel(II) complexes. *Polyhedron* **2010**, *29*, 574–580. [[CrossRef](#)]
57. *The Program BrukerSAINT*; Bruker AXS Inc.: Madison, WI, USA, 2012.
58. Sheldrick, G.M. *SADABS Software for Empirical Absorption Corrections*; University of Göttingen: Göttingen, Germany, 1996.
59. Sheldrick, G.M. SHELXT-integrated space-group and crystal-structure determination. *Acta Cryst.* **2015**, *A71*, 3–8. [[CrossRef](#)] [[PubMed](#)]
60. Farrugia, L.J. WinGX and Ortep for Windows: An update. *J. Appl. Cryst.* **2012**, *45*, 849–854. [[CrossRef](#)]
61. Macrae, C.F.; Bruno, I.J.; Chisholm, J.A.; Edgington, P.R.; McCabe, P.; Pidcock, E.; Rodriguez-Monge, L.; Taylor, R.J.; Van De Streek, J.; Wood, P.A. New features for the visualization and investigation of crystal structures. *J. Appl. Crystallogr.* **2008**, *41*, 466. [[CrossRef](#)]
62. Liang, X.-S.; Li, R.-D.; Wang, X.-C. Copper-catalyzed asymmetric annulation reactions of carbenes with 2-iminyl- or 2-acyl-substituted phenols: Convenient access to enantioenriched 2,3-dihydrobenzofurans. *Angew. Chem. Int. Ed.* **2019**, *58*, 13885–13889. [[CrossRef](#)]
63. Fekete, T.; Tumah, H.; Woodwell, J.; Truant, A.; Satischandran, V.; Axelrod, P.; Kreter, B. A comparison of serial plate agar dilution, Bauer-Kirby disk diffusion, and the Vitek AutoMicrobic system for the determination of susceptibilities of *Klebsiella spp.*, *Enterobacter spp.*, and *Pseudomonas aeruginosa* to ten antimicrobial agents. *Diagn. Microbiol. Infect. Dis.* **1994**, *18*, 251–258. [[CrossRef](#)]
64. Skehan, P.; Storeng, R.; Scudiero, D.; Monks, A.; McMahon, J.; Vistica, D.; Warren, J.T.; Bokesch, H.; Kenney, S.; Boyd, M.R. New colorimetric cytotoxicity assay for anticancer-drug screening. *J. Natl. Cancer Inst.* **1990**, *82*, 1107–1112. [[CrossRef](#)] [[PubMed](#)]
65. International Seed Testing Association. *International Rules for Seed Testing, Seed Science and Technology*; ISTA: Zurich, Switzerland, 1999; 334p.
66. Scott, S.J.; Jones, R.A.; Williams, W. Review of data analysis methods for seed germination. *Crop Sci.* **1984**, *24*, 1192–1199. [[CrossRef](#)]
67. Bharti, S.; Choudhary, M.; Mohan, B.; Rawat, S.P.; Sharma, S.R.; Ahmad, K. Syntheses, characterization, superoxide dismutase, antimicrobial, crystal structure and molecular studies of copper(II) and nickel(II) complexes with 2-((E)-(2,4-dibromophenylimino)methyl)-4-bromophenol as Schiff base ligand. *J. Mol. Struct.* **2017**, *1149*, 846–861. [[CrossRef](#)]
68. Geary, W.J. The use of conductivity measurements in organic solvents for the characterisation of coordination compounds. *Coord. Chem. Rev.* **1971**, *7*, 81–122. [[CrossRef](#)]

69. Devi, J.; Sharma, S.; Kumar, S.; Kumar, B.; Kumar, D.; Jindal, D.K.; Das, S. Synthesis, characterization, *in vitro* antimicrobial and cytotoxic studies of Co(II), Ni(II), Cu(II), and Zn(II) complexes obtained from Schiff base ligands of 1,2,3,4-tetrahydro-naphthalen-1-ylamine. *Appl. Organomet. Chem.* **2022**, *36*, e6760. [[CrossRef](#)]
70. Saechio, S.; Clerac, R.; Murray, K.S.; Phonsri, W.; Ruiz, E.; Harding, P.; Harding, D.J. Nickel(II) salicylaldimines: Re-visiting a classic. *Polyhedron* **2021**, *205*, 115321. [[CrossRef](#)]
71. Ramesh, R.; Maheswaran, S. Synthesis, spectra, dioxygen affinity and antifungal activity of Ru(III) Schiff base complexes. *J. Inorg. Biochem.* **2003**, *96*, 457–462. [[CrossRef](#)]
72. Abdolmaleki, S.; Yarmohammadi, N.; Adibi, H.; Ghadermazi, M.; Ashengroph, M.; Rudbari, H.A.; Bruno, G. Synthesis, X-ray studies, electrochemical properties, evaluation as *in vitro* cytotoxic and antibacterial agents of two antimony(III) complexes with dipicolinic acid. *Polyhedron* **2019**, *159*, 239–250. [[CrossRef](#)]
73. Ferraz, K.S.O.; Silva, N.F.; da Silva, J.G.; de Miranda, L.F.; Romeiro, C.F.D.; Souza-Fagundes, E.M.; Mendes, I.C.; Beraldo, H. Investigation on the pharmacological profile of 2,6-diacetylpyridine bis(benzoylhydrazone) derivatives and their antimony(III) and bismuth(III) complexes. *Eur. J. Med. Chem.* **2012**, *53*, 98–106. [[CrossRef](#)] [[PubMed](#)]
74. Kotian, A.; Kamat, V.; Naik, K.; Kokare, D.G.; Kumara, K.; Neratur, K.L.; Kumbhar, V.; Bhat, K.; Revankar, V.K. 8-Hydroxyquinoline derived p-halo N4-phenyl substituted thiosemicarbazones: Crystal structures, spectral characterization and *in vitro* cytotoxic studies of their Co(III), Ni(II) and Cu(II) complexes. *Bioorg. Chem.* **2021**, *112*, 104962. [[CrossRef](#)] [[PubMed](#)]
75. Taiz, L.; Zeiger, E. *Plant Physiology*, 5th ed.; Sinauer Associates Inc.: Sunderland, MA, USA, 2010; 782p.
76. Patel, M.N.; Patel, C.R.; Joshi, H.N. Metal-based biologically active compounds: Synthesis, characterization, DNA interaction, antibacterial, cytotoxic and SOD mimic activities. *Appl. Biochem. Biotechnol.* **2013**, *169*, 1329–1345. [[CrossRef](#)] [[PubMed](#)]
77. Dudhat, S.R.; Kulkarni, S. Application of Schiff bases and their metal complexes as insecticides and plant growth regulators- a review. *Int. J. Eng. Technol. Sci. Res.* **2018**, *5*, 740–743.

Disclaimer/Publisher's Note: The statements, opinions and data contained in all publications are solely those of the individual author(s) and contributor(s) and not of MDPI and/or the editor(s). MDPI and/or the editor(s) disclaim responsibility for any injury to people or property resulting from any ideas, methods, instructions or products referred to in the content.